Original Article

Inactivation of Poliovirus by Ozone and the Impact of Ozone on the Viral Genome[*]

JIANG Han Ji[^], CHEN Na[^], SHEN Zhi Qiang, YIN Jing, QIU Zhi Gang, MIAO Jing, YANG Zhong Wei, SHI Dan Yang, WANG Hua Ran, WANG Xin Wei, LI Jun Wen, YANG Dong[#], and JIN Min[#]

Department of Environment and Health, Tianjin Institute of Environmental & Operational Medicine, Key Laboratory of Risk Assessment and Control for Environment & Food Safety, Tianjin 300050, China

Abstract

Objective   To investigate the mechanisms underlying ozone-induced inactivation of poliovirus type 1 (PV1).

Methods   We used cell culture, long-overlapping RT-PCR, and spot hybridization assays to verify and accurately locate the sites of action of ozone that cause PV1 inactivation. We also employed recombinant viral genome RNA infection models to confirm our observations.

Results   Our results indicated that ozone inactivated PV1 primarily by disrupting the 5'-non-coding region (5'-NCR) of the PV1 genome. Further study revealed that ozone specifically damaged the 80-124 nucleotide (nt) region in the 5'-NCR. Recombinant viral genome RNA infection models confirmed that PV1 lacking this region was non-infectious.

Conclusion   In this study, we not only elucidated the mechanisms by which ozone induces PV1 inactivation but also determined that the 80-124 nt region in the 5'-NCR is targeted by ozone to achieve this inactivation.

Key words: Poliovirus; Poliomyelitis; Ozone; Disinfection

INTRODUCTION

Poliovirus (PV), the causative agent of poliomyelitis, invades the central nervous system and destroys motor nerve cells in the anterior horn of the spinal cord, consequently causing limb paralysis. In rare cases, it may even cause death by paralyzing muscles that control the throat or breathing[1]. PV was one of the most feared pathogens in industrialized countries during the 20th century, affecting hundreds of thousands of children every year *via* outbreaks during warm summer months. Although there are highly effective vaccines to control poliomyelitis, it remains endemic in a few countries, from which spread and outbreaks continue to occur worldwide[2-4].

PV is an enterovirus and is primarily transmitted through the fecal-oral and oral-oral route[1]. It can be excreted through patient feces, flowing into the aquatic environment, and consequently spreads via water. The resistance shown by enteroviruses in the aquatic environment (including survival time and endurance to various purification measures as well as disinfectants) is radically stronger than that shown by bacteria[5]. Lukasik et al. evaluated the effectiveness levels of various disinfectants in

[^]These authors contributed equally to this work.

[#]Correspondence should be addressed to JIN Min, E-mail: jinminzh@126.com; YANG Dong, E-mail: yangd8611@163.com

Biographical notes of the first authors: JIANG Han Ji, male, born in 1995, Master, majoring in microbiology; CHEN Na, female, born in 1985, Master, majoring in pharmaceutical engineering.

reducing or completely eradicating viable bacteria and viruses from the surfaces of strawberries, and they reported that free chlorine concentrations of as high as 300 ppm in washing water were needed to achieve disinfection[6]. Even after disinfection and contaminants being within acceptable levels in water, viruses can at times still be detected, of which enteroviruses are the most common. It has been reported that an individual needs to ingest just one detectable virus unit to develop an infection[7-10]. Using thorough disinfection methods is the only robust way to completely eradicate pathogens in water and thereby control infections; it is therefore imperative to study the effectiveness of different water disinfection methods to tackle pathogens such as PV type 1 (PV1).

Ozone has strong oxidizing properties and has been widely used in recent years for disinfecting drinking water[11-12]. The speed of disinfection is very fast, and the inactivation effect of ozone is better than that of disinfectants such as chlorine, chloramines, and chlorine dioxide (ClO_2); ozone can also oxidize and degrade organic substances in water[13-15]. The remaining ozone in water can naturally decompose so that the dissolved oxygen content in the effluent is high, the burden on the receiving water body is reduced, and the quality of water can be improved[16-17].

Roy et al. reported that ozone damages two of the four polypeptide chains present in the viral capsid of PV1; however, protein coat alteration does not significantly impair the adsorption of the virus or alter the integrity of viral particles; damage to viral nucleic acids by ozone was the foremost reason for PV1 inactivation[18]. Considering the different functions of each region of viral nucleic acids, the target sequences in the PV1 genome can be segregated into a 5'-non-coding region (NCR), coding region, 3'-NCR, and poly(A) tail[19]. Simonet and Gantzer determined that the 5'-NCR of the PV1 genome gets damaged upon ClO_2 treatment, resulting in PV1 inactivation[20]. Moreover, Bhattacharya et al. reported that when RT-PCR was used to evaluate the changes in hepatitis A virus (HAV) infectivity after exposing viral samples to heat or UV irradiation, PCR signals exclusively generated by primers designed in the 5'-NCR of the viral genome helped discriminate between infectious and non-infectious HAV[21]. In our previous study, we demonstrated that ClO_2 induces PV1 inactivation by damaging the 40-80 nucleotide (nt) region in the 5'-NCR of the viral genome[22]. Nevertheless, when PV1 is disinfected with ozone, the site of action of ozone in the 5'-NCR of the viral genome remains unclear. In addition, with an increase in the demand to develop molecular biological techniques such as PCR and quantitative real-time PCR to investigate the contamination of water by infectious viruses, it has become crucial to investigate the relationship between PV1 infection and integrity of the viral genome upon exposure to disinfectants[23].

In this study, we used cell culture, long-overlapping RT-PCR, and spot hybridization assays to verify and accurately locate the sites of action of ozone in the 5'-NCR of the viral genome; we confirmed our observations by employing recombinant viral genome RNA infection models. We hypothesized that if the inactivation of viruses by disinfectants is based on viral genomic damage, molecular biological techniques should be able to effectively evaluate the disinfection effect as they strictly depend on the integrity of target nucleic acids, which are used as a template.

MATERIALS AND METHODS

Virus and Cells

Attenuated PV1 strain LSc/2ab was obtained from the National Institute for Biological Standards and Control (UK). Viruses were propagated and titrated using Vero cells. Cultures of PV1-infected cells were harvested after the development of extensive cytopathic effects (usually 24 h post-inoculation). Cells were subjected to three freeze-thaw cycles to release the virus, followed by centrifugation at 1,200 ×g for 10 min at 48 °C to remove cell debris. The supernatant was then assayed for infectious PV1 and found to contain $10^{7.25}$ tissue culture infective dose/mL[22]. The viral suspension was stored at -80 °C. Before use, the suspension was thawed, sonicated for 30 s at 20 kHz (150 W), and filtered through a 0.22-μm pore size membrane to remove any large clumps or aggregates of PV1.

Preparation and Concentration Determination of Ozone Water

Ozone was generated using an air source; ozone generated by the ozone-generating equipment was introduced into a glass cylinder containing 100 mL distilled water, and tail gas was absorbed using a surplus of sodium sulfite solution. Immediately, 2.5 mL potassium iodide and (1:3) sulfuric acid were added to the ozone water; the solution was

thoroughly mixed and incubated for 5 min in the dark. Then, titration was performed using 0.01 mol/L $Na_2S_2O_3$. When a pale-yellow color was obtained, 1 mL of 5 g/L starch was added. The solution consequently turned blue; titration was continued until the solution became colorless. The titration volume of $Na_2S_2O_3$ was used to calculate the concentration of ozone[24].

Disinfection via Ozone

The viral suspension was added to 100 mL water sample at 20 °C and thoroughly mixed to obtain a concentration of 10^6 plaque-forming units (PFU)/L. The flow rate of ozone was 0.5 L/min, and the ventilation time was set to 0, 30, 60, 90, 105, and 120 s[24]. The ozone-sterilized viral suspension was connected to the Vero cells to detect any live viruses in the sample. The concentration of ozone in the water sample at each timepoint was measured by the above method, and three replicates were used for each timepoint.

PV1 Infection

The sterilized viral suspension was diluted and inoculated into a 25-cm² cell culture flask containing a single layer of Vero cells; three replicates were used for each timepoint. After mixing 2× 1640 maintenance medium and 2% agar in equal volumes, it was added to a cell culture flask to cover the cells to form a solid medium, and the number of plaques formed was counted after 2 days of incubation in a cell culture incubator. PV1 concentration was subsequently calculated from the number of plaques formed and expressed as PFU.

$$PFU = \text{Dilution factor} \times \frac{P1+P2+P3}{n} \times \frac{1}{v} \quad (1)$$

In the above formula, *P* represents the number of plaques formed, *n* is the number of cell culture flasks, and *v* is the inoculum volume (mL).

RNA Extraction

Viral RNA was extracted and purified using RNeasy columns (Qiagen, USA), according to manufacturer's instructions.

Primers and RT-PCR

Different regions of the viral genome were amplified using RT-PCR. Primers used for detecting viral genome sites that were damaged by ozone are listed in Supplementary Table S1, available in www.besjournal.com.

First, the extracted RNA was reverse transcribed with random primers and oligo(dT) primers using PrimeScript™ II First Strand cDNA Synthesis Kit (Takara 6210A), as per manufacturer's instructions. The obtained cDNA was then used as a template to amplify different target regions with corresponding primers. Each 20 μL reaction mixture included 2.5 μL cDNA template, 12.5 μL Taq polymerase, 0.5 μL primers (10 μmol/L), and 4 μL distilled water. The thermal cycler conditions were as follows: 1 cycle of initial denaturation at 94 °C for 3 min, 30 cycles of denaturation at 94 °C for 30 s, annealing at 55 °C for 30 s, and extension at 72 °C for 60 s, followed by a final elongation step at 72 °C for 7 min. All PCR products were analyzed by electrophoresis using 1.5% (w/v) agarose gels stained with ethidium bromide.

Probes and Spot Hybridization

Spot hybridization assays were performed using biotinylated probes[25]. A nitrocellulose membrane was pre-soaked in 2× saline sodium citrate (SSC) buffer for 2 h and air-dried before use. PV1 RNA suspensions were mixed with an equal volume of RNA fixative, incubated at 68 °C, and then chilled in an ice bath. Two volumes of 20× SSC were subsequently added to the mixture to establish an RNase-free environment. A pencil was used to create marks on the membrane, and viral RNA samples were dot blotted. The membrane was placed on a clean filter paper and then in a nucleic acid cross-linking instrument, and irradiated with a UV lamp to immobilize the RNA on the membrane. Subsequently, the membrane was completely immersed in a hybridization solution to facilitate pre-hybridization. The hybridization solution and probes were mixed in equal volumes, and this was applied to the locations marked on the membrane. The membrane was then placed in a hybridization medium to facilitate hybridization, and it was then washed using a washing buffer. After drying the membrane, 2 μL horseradish peroxidase (HRP)-biotin was diluted in 2 mL hybridization solution, and this was carefully applied to the defined RNA sample locations on the membrane. Once dried, the membrane was placed in the hybridization solution, incubated at 37 °C, and washed using the washing buffer. One drop of 3,3'-diaminobenzidine and 37% H_2O_2 were added to 2 mL phosphate buffer saline (PBS) and uniformly mixed, and the membrane was placed in this solution at room temperature to facilitate color development. The membrane was finally placed on a filter paper and allowed to dry

before a photograph was taken. The probes used for spot hybridization assays are shown in Supplementary Table S2, available in www.besjournal.com.

Construction of Damaged PV1 RNA

Viral cDNA was synthesized *in vitro* and transcribed using RNA polymerase into RNA, which was used to infect cells, ultimately resulting in the synthesis of infectious PV[26]. RNA extraction and reverse transcription were performed as previously described. Primers used to construct damaged PV1 RNA are listed in Supplementary Table S3, available in www.besjournal.com.

Each 50 µL reaction mixture contained 1 µL cDNA template, 1 µL primers (5 µmol/L), 1 µL Trans HiFi (10 U/µL), 5 µL 10× HiFi buffer, 5 µL dNTPs (2.5 mmol/L), and 36 µL distilled water. The thermal cycler conditions were as follows: 1 cycle of initial denaturation at 94 °C for 3 min, 30 cycles of denaturation at 94 °C for 30 s, annealing at 53 °C for 30 s, and extension at 72 °C for 60 s, followed by a final elongation step at 72 °C for 10 min. All PCR products were analyzed by electrophoresis using 1.5% (w/v) agarose gels stained with ethidium bromide.

The recovered PV1 DNA fragment was treated with *EcoRI* to form a sticky end between the 3'-end of the upstream fragment and the 5'-end of the downstream fragment of the injury site. Each 100 µL reaction mixture included 25 µL 10× *EcoRI* buffer, 10 µL template DNA, 10 µL *EcoRI*, and 55 µL ultrapure water. The reaction was performed at 37 °C for 2 h, and the DNA was precipitated using absolute ethanol. The upstream and downstream DNA fragments were ligated with T4 DNA ligase to obtain PV1 double-stranded genomic DNA that was damaged in the 5'-NCR partial region.

After constructing the recombinant PV1 genome, T7 RNA polymerase was used to synthesize recombinant viral genomic RNAs *in vitro* using the newly constructed PV1 genomic DNA with T7 bacteriophage transcript promoter. The reaction mixture comprised 10 µL 10× T7 RNA polymerase buffer, 10 µL dNTPs (2.5 mmol/L), 20 µL DTT (50 mmol/L), 2.5 µL RNase inhibitor (40 U/µL), 10 µL PV1 template DNA (20 ng/mL), and 5-25 U T7 RNA polymerase; DEPC water was used to obtain a final volume of 100 µL. After incubation at 37 °C for 30-60 min, 10 U of RNase-free DNase I and RNase inhibitor were added to 1 U/µL, followed by incubation at 37 °C for 10 min. The solution was then transferred to a column and total RNA was extracted.

Infectivity Determination of Recombinant PV1 Genomic RNAs

The infectivity of recombinant PV1 genomic RNAs was analyzed using plaque-forming assays[27]. Vero cells were grown on a 25-cm^2 square to form a monolayer and washed twice with PBS in DEPC water. Viral RNA was serially diluted 10-fold with Hanks balanced salt solution containing 1 mg/mL DEAE-dextran, and chilled for 30 min in an ice batch. Subsequently, 1 mL DEPC-treated PBS was added to each cell culture well, and 200 µL of different concentrations of gradient RNA solution was added to each well. The culture flask was thoroughly stirred; two wells were inoculated for each dilution gradient. After adsorption for 30 min at room temperature, it was mixed with 2× 1640 maintenance medium and 2% agarose and then spread into a cell culture plate. At the same time, PV1 RNA extracted from viral particles was used as a control to infect Vero cells, and infectivity of the synthesized PV1 RNA was compared.

If no plaques formed in the first round of transfection, the culture supernatant was used to re-infect Vero cells, and the inoculation cycle was repeated three times. RNA isolated from the supernatant of the third inoculation was extracted using the extraction method described earlier, and RT-PCR was performed using the primer pair listed in Supplementary Table S1 to exclude the possibility of false-negative or latent infection.

RESULTS

Relationship between PV1 Inactivation by Ozone and Antigenic Injury

The concentration of ozone in water (mg/L) increased with an increase in ventilation time, and the concentration became stable after saturation (Supplementary Table S4, available in www.besjournal.com).

As ozone-depleting substances were present in the water body containing PV1, the concentration of ozone in water was 0 mg/L when ventilation was started. When equilibrium was reached, the concentration of ozone increased with ventilation time. Time- and dose-dependent effects of ozone on PV1 inactivation and antigenic injury were observed. An increase in the concentration of ozone or ventilation time resulted in a decline in PV1 survival rate and an increase in the degree of antigenic injury (Figure 1). The time required for ozone to inactivate

PV1 was very short-PV1 was completely eradicated by ozone upon disinfecting water for 105-120 s (Supplementary Table S5, available in www.besjournal.com).

Primer Validation

Primers designed to amplify the full-length PV1 genome were validated by RT-PCR using untreated (native) PV1 RNA as a template. All expected targets, 6 long and 3 short fragments, were amplified successfully (Supplementary Figure S1, available in www.besjournal.com). Furthermore, the 6 long fragment sequences were verified by sequencing and aligning to the 7441-nt region, which were demonstrated by BLAST to be identical to those published earlier[28].

Effect of Ozone on Infectivity and Genomic Integrity of PV1

PV1 infectivity was completely inhibited upon disinfecting the water sample with ozone for 105 s. When water samples exposed to different disinfection times were separately subjected to RT-PCR to study the PV1 genome, region-specific sensitivities to ozone were revealed. The first region lost to detection was the 1-1,297 nt region in the 5'-NCR (Figure 2). Further study was conducted to elucidate the relationship between damage to the PV1 genome and changes to viral infectivity, and the obtained results showed that the 1-124 nt region was damaged (Figure 3). As ozone concentration or disinfection time increased, other regions of the genome were damaged after 120 s of disinfection. These findings indicated that different regions of the PV1 genome have different resistance to ozone. The 1-124 nt region was the most sensitive and its damage was consistent with the disappearance of PV1 infectivity. The rest of the genome showed stronger resistance, and damage to other regions, as evident from the data presented in Table 1, was not completely consistent with changes to PV1 infectivity. These observations indicated that ozone-induced inactivation of PV1 occurs *via* damage to the 1-124 nt region in the 5'-NCR.
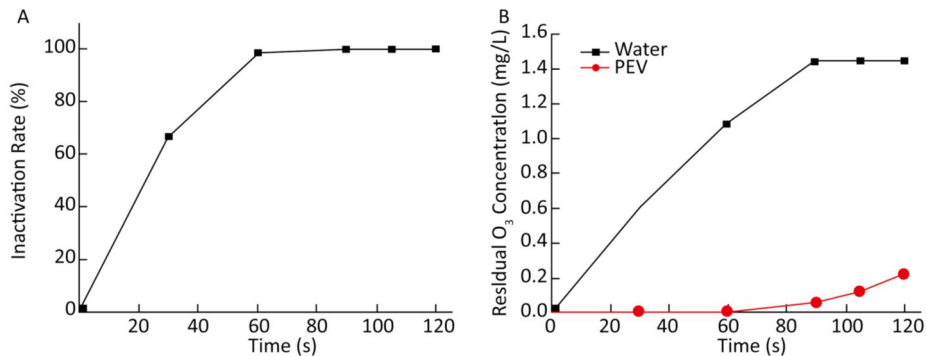

Figure 1. (A) Ozone-induced changes of PV1 inactivation rate. (B) Dissolved concentration curve of ozone in 100 mL distilled water and 100 mL PV1-containing water. The baseline conditions were: initial concentration of PV1 was 106 PFU/L in 100 mL water sample, ventilation flow was 0.5 L/min, and temperature was 20 °C.

Table 1. Damage to PV1 RNA by Different Concentrations of Ozone

Ventilation Time (s)	Ozone Concentration (mg/L)	Infectivity	Nucleic Acid Region (nt)				
			1-1,297	1-124	108-679	669-1,274	939-7,441
0	0	+	+	+	+	+	+
30	0.60	+	+	+	+	+	+
60	1.08	+	+	+	+	+	+
90	1.44	+	+	+	+	+	+
105	1.44	-	-	-	+	+	+
120	1.44	-	-	-	-	-	-

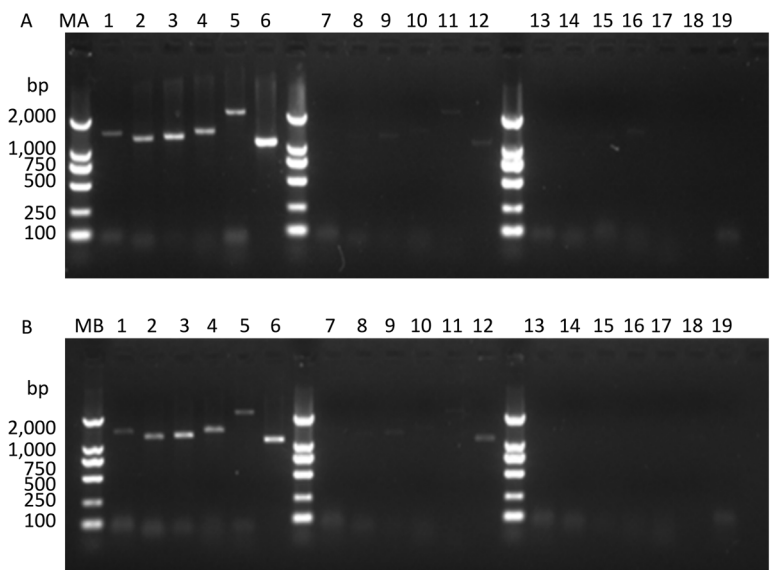***Note.*** +, Positive result; -, Negative result in replicate experiments (*n* = 3).

Figure 2. Detection of RT-PCR products in virus-containing water samples sterilized by ozone at different times. (A) The RT-PCR products of PV1 cDNA synthesized with random primers. (B) The RT-PCR products of PV1 cDNA synthesized with oligo-dT primers. Lanes 1-6 were Positive controls, correspond to the amplification products of primer set 1 to primer set 6, respectively. Lanes 7-12: Disinfection time of 105 s, lanes 13-18: Disinfection time of 120 s, lane 19 was a negative control for primer set 1. Lanes MA and MB, DL2000 DNA markers (2,000, 1,000, 750, 500, 250, and 100 bp).
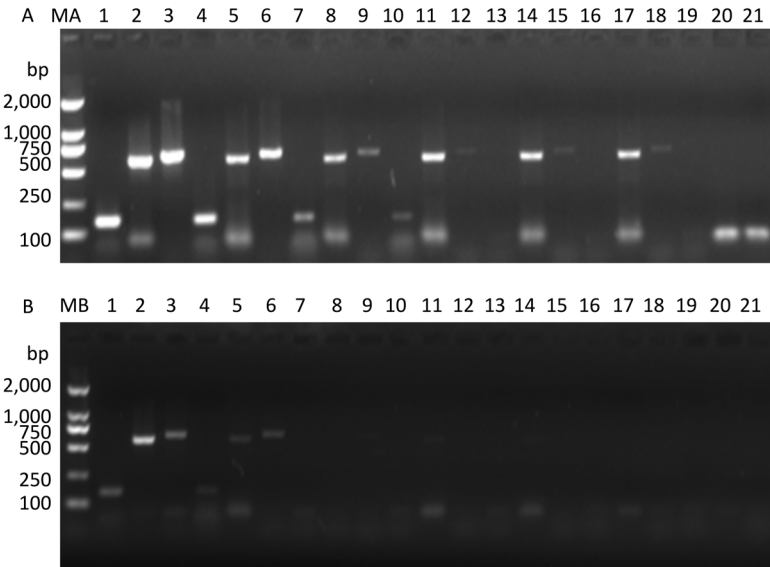

Figure 3. Precise detection of RT-PCR products in virus-containing water samples sterilized by ozone at different times. (A) The RT-PCR products of PV1 cDNA in the 5'-NCR synthesized with random primers. (B) The RT-PCR products of PV1 cDNA in the 5'-NCR synthesized with oligo-dT primers. Lanes 1-3 were positive controls, correspond to the amplification products of primer sets 5'-1/1F, 5'-2F/5'-2R, and 5'-3/1R, respectively. Lanes 4-6: Disinfection time of 30 s, lanes 7-9: Disinfection time of 60 s, lanes 10-12: Disinfection time of 90 s, lanes 13-15: Disinfection time of 105 s, lanes 16-18: Disinfection time of 120 s, lane 19-21 were negative controls. Lanes MA and MB, DL2000 DNA markers (2,000, 1,000, 750, 500, 250, and 100 bp).

Fine Mapping of 5'-NCR Sensitive Targets in the PV1 Genome

Spot hybridization assays reportedly have better sensitivity and the detection effect is ideal. Probe 2 was used for spot hybridization. The method could detect 17 PFU/mL of viral RNA (Supplementary Figure S2, available in www.besjournal.com).

Viral RNA was extracted from PV1 after disinfection using ozone for 0, 90, 105, and 120 s, and spot hybridization assay was used to accurately locate the 5'-NCR sensitive targets in the PV1 genome. The 5'-NCR loci corresponding to probe 3 (80-124 nt) was the most sensitive to damage by ozone (Figure 4). Moreover, loss of the integrity of this small 45-nt region was accompanied by loss of PV1 infectivity (Supplementary Table S6, available in www.besjournal.com).

Relationship between Loss of Infectivity and Genomic Damage

PV1 genomic DNA and RNA lacking different target sequences were constructed and verified using RT-PCR (Supplementary Figure S3, available in www.besjournal.com). The plaque-forming assay of the corresponding recombinant viral genomes indicated that the full-length viral genomic RNA had high infectivity (Figure 5), whereas the viral genome lacking the 80-124 nt and 1-124 nt regions had no infectivity (Figure 6).
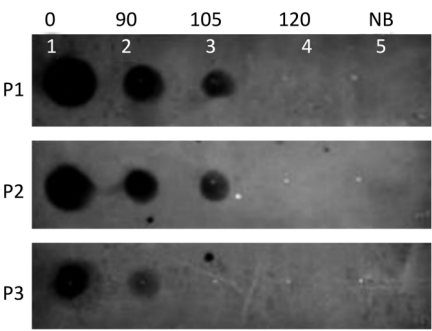
Figure 4. Spot hybridization assay to determine ozone-sensitive regions in the 5'-NCR of the PV1 genome (n = 3). PV1 RNA was cross-linked on a membrane and hybridized with biotinylated probes targeting different regions. Spot 5 corresponds to the negetive control. Spots 1-4 correspond to RNA from PV1 treated with ozone for 0, 90, 105, and 120 sec. Spots were detected with probes to P1 (1-40 nt), P2 (40-80 nt), P3 (80-124 nt) region.
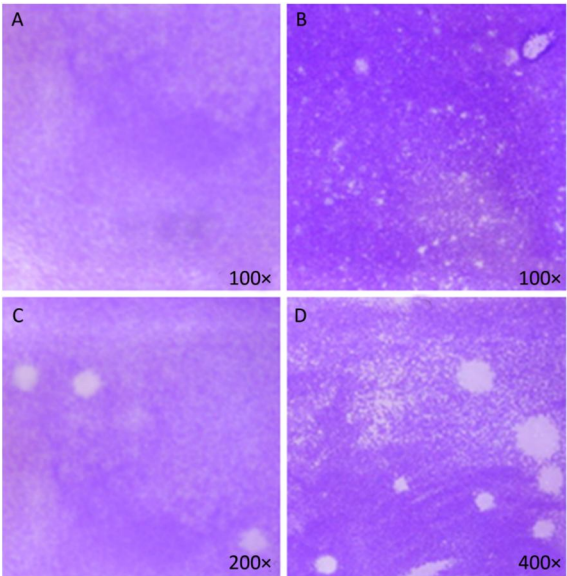
Figure 5. Plaque-forming cell assay using full-length viral genomic RNA and viral particles (n = 3). (A) Negative control, no PV1 RNA was inoculated, (B) Integrated virus RNA, (C) Complete virus particle (17 PFU), (D) Complete virus particle (170 PFU).
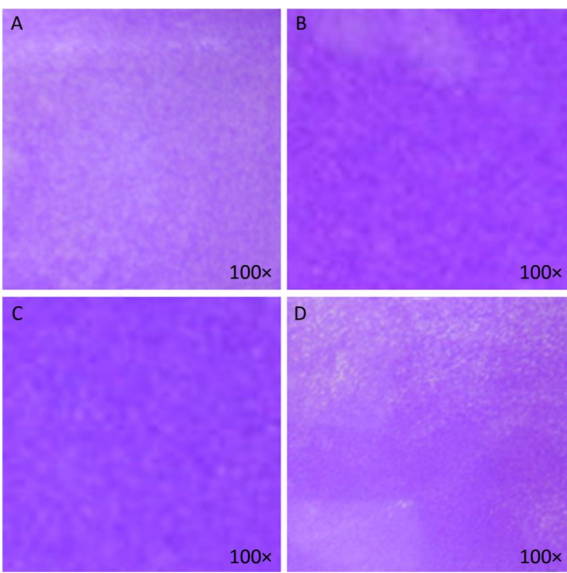
Figure 6. Plaque-forming cell assay to determine infectivity of recombinant PV1 RNA with sensitive targets deleted (n = 3). Recombinant viral RNA were inoculated into the culture supernatant of Vero cells. (A) RNA lacking 1-124 nt of 5'-NCR, (B) is parallel to, (C) RNA lacking 80-124 nt of 5'-NCR, (D) is parallel to C.

Viral nucleic acids were not detected in the culture supernatants from inoculated cells infected with recombinant viruses, indicating loss of infectivity when the 80-124 nt and 1-124 nt regions were missing.

DISCUSSION

Ozone is an effective disinfectant and is widely used to purify drinking water[12]. In this study, we found that the effect of ozone on PV1 infectivity was both time- and dose-dependent, and PV1 could be completely eradicated after ozone disinfection for 105 s. It has been previously reported that PV1 infectivity is completely inhibited upon treatment with 0.2 mg/L ClO_2 for 12 min, 0.4 mg/L ClO_2 for 8 min, or 0.8 mg/L ClO_2 for 4 min[22]. This proves that ozone is more effective as a disinfectant than ClO_2. When ozone is used to disinfect drinking water, the concentration of ozone needed is very low too. On disinfecting water with ozone at a mass concentration of 0.4 mg/L for 4 min, effective disinfection can be achieved[29]. These findings indicate that ozone has a very broad prospect as a water disinfectant.

Researchers have suggested that ozone inactivates viruses by destroying viral nucleic acids or capsid proteins. Moore and Margolin published a study in which PV1 was treated with chlorine, ClO_2, ozone, and UV irradiation to determine the effectiveness of each disinfectant, and they could detect viral nucleic acids even after PV1 infectivity was completely eliminated. They speculated that viral inactivation may be associated with capsid protein damage[30]. However, Roy et al. found that although ozone can destroy the capsid protein of PV1, viral infectivity still exists. The destruction of the viral nucleic acid by ozone is the main reason for PV1 inactivation[18].

Although most related studies indicate that ozone-induced PV1 inactivation is associated with damage to the viral genome, specific sequences targeted by ozone within the viral genome have not yet been identified. Here we used RT-PCR and spot hybridization assays to identify the sites of action of ozone in the 5'-NCR of the viral genome. Our results indicated that the genetic target damaged by ozone was mainly located in the 80-124 nt region in the 5'-NCR. Moreover, our infection model confirmed that RNA lacking the 80-124 nt region in the 5'-NCR caused complete loss of infectivity. The obtained results also demonstrated that viral nucleic acids could be detected after complete elimination of viral infection and that all detectable regions were located in the coding region of the viral genome, indicating that this region is most resistant to the effect of disinfectants.

Simonet and Gantzer also reported that the 5'- and 3'-NCR of the PV1 genome appeared to be the most sensitive to ClO_2 treatment[31]. In one of our previous study, Jin et al. determined that the genetic target damaged by ClO_2 in the 5'-NCR is mainly located in the 40-80 nt region, resulting in PV1 inactivation[22]. With regard to other enteroviruses, Jin et al. reported that ClO_2 inactivates EV71 by disrupting the 1-118 nt region in the 5'-NCR[5]; Li et al. also determined that the loss of ClO_2-induced HAV infectivity is associated with damages to the 5'-NCR[32].

The 5'-NCR of the PV1 genome is mainly associated with viral transcription, replication, translation, and invasion[33]. The nucleotide sequence of this region contains a high degree of mutual complementarity between strands, which supports the formation of hairpin or stem-loop secondary structures. The 5'-NCR has six stem-loop domains, representing two functional elements. Domain I is the 1-80 nt region that is a cloverleaf structure and associated with the replication of viral nucleic acids[34-35]. This region is bound by the polyC-binding protein and viral protease-polymerase 3CD to form the ribonucleoprotein complex B[36], which catalyzes the synthesis of plus-strand RNA of viruses. Domains II-VI in the 130-610 nt region are associated with viral protein synthesis. Defined as an internal ribosomal entry site, they directs ribosomes near the initiation codon for RNA translation, improving the efficiency of translation[33,37-38].

The software-predicted secondary structure showed that the 80-124 nt region is free single-stranded and linked to domain II. Interrelated secondary structures may have a decisive influence on viral replication, which may be attenuated during the normal passage of the virus due to variations in certain bases in the secondary hairpin or stem-loop structure[39]. Deletion of the stem-loop structure region can stop the virus from multiplying[40]. From an energy point of view, the energy provided by ozone acts on the nucleic acid strand, and as the nucleotides of the single-stranded region are mainly hydrogen bonded at a lower energy level, the energy required to break the single-strand hydrogen bond connection is minimal. Free single-strand breaks between domains I and II can cause breaks or base

mutations, leading to alterations in the secondary structure. Fragmentation of such bases directly results in the deletion of domain I, causing loss of viral infectivity.

Traditional methods to detect viruses that involve cell culture are complex and time-consuming, and therefore, they are not feasible for evaluating subtle genetic or molecular effects of disinfectants. Spot hybridization assays and RT-PCR are rapid and scalable but limited in their ability to distinguish between active and inactive viruses[30]. A couple of studies that involved the use of RT-PCR to determine PV1 status after treatment with UV irradiation, chlorine, HCl, and NaOH reported that the detected viral nucleic acids did not correspond with the loss of viral infectivity evidenced in cell culture[41-42]. Likewise, Lim et al. reported that both long and short template RT-PCR assays markedly underestimated the extent of virus inactivation in comparison to plaque-forming assays[43]. Consequently, majority of researchers presumed that as RT-PCR or nucleic acid probes cannot distinguish between inactive and active viruses, these methods could overestimate viral infectivity and are thus unsuitable for a robust evaluation of the effects of disinfectants.

Here we hypothesized that if the inactivation of viruses by disinfectants is based on viral genomic damage, molecular biological techniques should be able to effectively evaluate the effects of disinfectants as these techniques strictly depend on the integrity of target nucleic acids, which are used as a template. Previous researchers only detected target nucleic acid fragments in the coding region of the viral genome, whereas our results suggest that this region harbors the strongest resistance to disinfectants. Furthermore, previous studies have confirmed that the target of disinfectant-induced PV1 inactivation is located in the 5'-NCR, rather than in the coding region[31-32]. Thus, it was presumed that if sequences sensitive to disinfectants were instead used as the detection targets for inactivated viruses, it would be feasible to evaluate the disinfection effect by employing molecular biological techniques. The overall results of this study support this view.

In conclusion, we evaluated the mechanisms by which ozone inactivates PV1 and determined that PV1 inactivation by ozone is associated with damage to the viral genome, rather than to the capsid protein. Our results also indicate that ozone-sensitive genomic targets are located within the 5'-NCR of the PV1 genome.

CONFLICTS OF INTEREST

The authors declare no competing financial interests.

REFERENCES

1. Lévêque N, Semler BL. A 21st century perspective of poliovirus replication. PLoS Pathog, 2015; 11, e1004825.
2. Alam MM, Sharif S, Shaukat S, et al. Genomic Surveillance Elucidates Persistent Wild Poliovirus Transmission During 2013-2015 in Major Reservoir Areas of Pakistan. Clin Infect Dis, 2016; 62, 190-8.
3. Famulare M. Has Wild Poliovirus Been Eliminated from Nigeria. PLoS One, 2015; 10, e0135765.
4. Moran-Gilad J, Kaliner E, Gdalevich M, et al. Public health response to the silent reintroduction of wild poliovirus to Israel, 2013-2014. Clin Microbiol Infect, 2016; 22, S140-S145.
5. Jin M, Shan J, Chen Z, et al. Chlorine dioxide inactivation of enterovirus 71 in water and its impact on genomic targets. Environ Sci Technol, 2013; 47, 4590-7.
6. Lukasik J, Bradley ML, Scott TM, et al. Reduction of poliovirus 1, bacteriophages, Salmonella montevideo, and Escherichia coli O157:H7 on strawberries by physical and disinfectant washes. J Food Prot, 2003; 66, 188-93.
7. Tree JA, Adams MR, Lees DN. Chlorination of indicator bacteria and viruses in primary sewage effluent. Appl Environ Microbiol, 2003; 69, 2038-43.
8. Nuanualsuwan S, Mariam T, Himathongkham S, et al. Ultraviolet inactivation of feline calicivirus, human enteric viruses and coliphages. Photochem Photobiol, 2002; 76, 406-10.
9. Apaire-Marchais V, Robertson BH, Aubineau-Ferre V, et al. Direct sequencing of hepatitis A virus strains isolated during an epidemic in France. Appl Environ Microbiol, 1995; 61, 3977-80.
10. Churn CC, Bates RC, Boardman GD. Mechanism of chlorine inactivation of DNA-containing parvovirus H-1. Appl Environ Microbiol, 1983; 46, 1394-402.
11. LYK N, RMB F, VRDS F, et al. Pre-ozonation of source water: Assessment of efficacy against Giardia duodenalis cysts and effects on natural organic matter. Chemosphere, 2019; 214, 764-70.
12. von GU. Oxidation Processes in Water Treatment: Are We on Track. Environ Sci Technol, 2018; 52, 5062-75.

13. Dong S, Massalha N, Plewa MJ, et al. The impact of disinfection Ct values on cytotoxicity of agricultural wastewaters: Ozonation vs. chlorination. Water Res, 2018; 144, 482-90.

14. Wang H, Hu C, Zhang S, et al. Effects of O3/Cl2 disinfection on corrosion and opportunistic pathogens growth in drinking water distribution systems. J Environ Sci, 2018; 73, 38-46.

15. Önnby L, Salhi E, McKay G, et al. Ozone and chlorine reactions with dissolved organic matter - Assessment of oxidant-reactive moieties by optical measurements and the electron donating capacities. Water Res, 2018; 144, 64-75.

16. Tamaki M, Kobayashi F, Ikeura H, et al. Disinfection by Ozone Microbubbles Can Cause Morphological Change of Fusarium oxysporum f. sp. melonis Spores. Plant Pathol J, 2018; 34, 335-40.

17. Ofori I, Maddila S, Lin J, et al. Ozone initiated inactivation of Escherichia coli and Staphylococcus aureus in water: Influence of selected organic solvents prevalent in wastewaters. Chemosphere, 2018; 206, 43-50.

18. Roy D, Wong PK, Engelbrecht RS, et al. Mechanism of enteroviral inactivation by ozone. Appl Environ Microbiol, 1981; 41, 718-23.

19. Kitamura N. [Genome structure of poliovirus (author's transl)]. Seikagaku, 1982; 54, 151-6.

20. Simonet J, Gantzer C. Inactivation of poliovirus 1 and F-specific RNA phages and degradation of their genomes by UV irradiation at 254 nanometers. Appl Environ Microbiol, 2006; 72, 7671-7.

21. Bhattacharya SS, Kulka M, Lampel KA, et al. Use of reverse transcription and PCR to discriminate between infectious and non-infectious hepatitis A virus. J Virol Methods, 2004; 116, 181-7.

22. Jin M, Zhao ZG, Wang XW, et al. The 40-80 nt region in the 5'-NCR of genome is a critical target for inactivating poliovirus by chlorine dioxide. J Med Virol, 2012; 84, 526-35.

23. Zaidi SS, Asghar H, Sharif S, et al. Poliovirus Laboratory Based Surveillance: An Overview. Methods Mol Biol, 2016; 1387, 11-8.

24. Katzenelson E, Biedermann N. Disinfection of viruses in sewage by ozone. Water Res, 1976; 10, 629-31.

25. Chatterjee NK, Kaehler M, Deibel R. Detection of enteroviruses using subgenomic probes of Coxsackie virus B4 by hybridization. Diagn Microbiol Infect Dis, 1988; 11, 129-36.

26. Cello J, Paul AV, Wimmer E. Chemical synthesis of poliovirus cDNA: generation of infectious virus in the absence of natural template. Science, 2002; 297, 1016-8.

27. Nuanualsuwan S, Cliver DO. Infectivity of RNA from inactivated poliovirus. Appl Environ Microbiol, 2003; 69, 1629-32.

28. Nomoto A, Omata T, Toyoda H, et al. Complete nucleotide sequence of the attenuated poliovirus Sabin 1 strain genome. Proc Natl Acad Sci USA, 1982; 79, 5793-7.

29. Camel V, Bermond A. The use of ozone and associated oxidation processes in drinking water treatment. Water Res, 1998; 32, 3208-22.

30. Moore NJ, Margolin AB. Efficacy of Nucleic Acid Probes for Detection of Poliovirus in Water Disinfected by Chlorine, Chlorine Dioxide, Ozone, and UV Radiation. Appl Environ Microbiol, 1994; 60, 4189-91.

31. Simonet J, Gantzer C. Degradation of the Poliovirus 1 genome by chlorine dioxide. J Appl Microbiol, 2006; 100, 862-70.

32. Li JW, Xin ZT, Wang XW, et al. Mechanisms of inactivation of hepatitis A virus in water by chlorine dioxide. Water Res, 2004; 38, 1514-9.

33. Souii A, Ben MM, Gharbi J. Role of RNA structure motifs in IRES-dependent translation initiation of the coxsackievirus B3: new insights for developing live-attenuated strains for vaccines and gene therapy. Mol Biotechnol, 2013; 55, 179-202.

34. Moustafa IM, Gohara DW, Uchida A, et al. Conformational Ensemble of the Poliovirus 3CD Precursor Observed by MD Simulations and Confirmed by SAXS: A Strategy to Expand the Viral Proteome. Viruses, 2015; 7, 5962-86.

35. Harris KS, Xiang W, Alexander L, et al. Interaction of poliovirus polypeptide 3CDpro with the 5' and 3' termini of the poliovirus genome. Identification of viral and cellular cofactors needed for efficient binding. J Biol Chem, 1994; 269, 27004-14.

36. Ogram SA, Spear A, Sharma N, et al. The 5'CL-PCBP RNP complex, 3' poly(A) tail and 2A(pro) are required for optimal translation of poliovirus RNA. Virology, 2010; 397, 14-22.

37. Schmid M, Wimmer E. IRES-controlled protein synthesis and genome replication of poliovirus. Arch Virol Suppl, 1994; 9, 279-89.

38. Fitzgerald KD, Semler BL. Re-localization of cellular protein SRp20 during poliovirus infection: bridging a viral IRES to the host cell translation apparatus. PLoS Pathog, 2011; 7, e1002127.

39. Muslin C, Joffret ML, Pelletier I, et al. Evolution and Emergence of Enteroviruses through Intra- and Inter-species Recombination: Plasticity and Phenotypic Impact of Modular Genetic Exchanges in the 5' Untranslated Region. PLoS Pathog, 2015; 11, e1005266.

40. Viktorova EG, Khattar S, Samal S, et al. Poliovirus Replicon RNA Generation, Transfection, Packaging, and Quantitation of Replication. Curr Protoc Microbiol, 2018; 48, 15H.4.1-15H.4.15.

41. Ma JF, Straub TM, Pepper IL, et al. Cell culture and PCR determination of poliovirus inactivation by disinfectants. Appl Environ Microbiol, 1994; 60, 4203-6.

42. Maier, Tougianidou, Wiedenmann, et al. Detection of poliovirus by cell culture and by PCR after UV disinfection. Water Sci Technoly, 1995; 31, 141-5.

43. Lim MY, Kim JM, Ko G. Disinfection kinetics of murine norovirus using chlorine and chlorine dioxide. Water Res, 2010; 44, 3243-51.
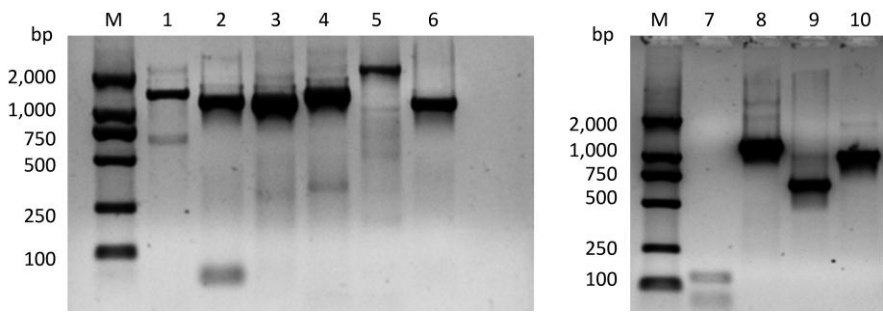
Supplementary Figure S1. Validation of primers designed to target different regions in the PV1 genome. Lane M is DL2000 DNA markers (2,000 bp, 1,000 bp, 750 bp, 500 bp, 250 bp, 100 bp); lanes 1-6 are the amplification products of the primer set 1 to the primer set 6; lanes 7-10 are the amplification product of the primer set 1, 5'-1/1F, 5'-2F/5'-2R, 5'-3/1R.
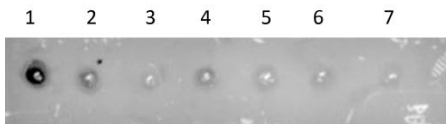
Supplementary Figure S2. Sensitivity verification of the spot hybridization assay (n = 3). PV1 RNA was cross-linked on a membrane and hybridized with probe 2. Spot 1, positive control; spots 2-, PV1 detection concentration of 1.7×10^6-1.7×10^1 PFU/mL.
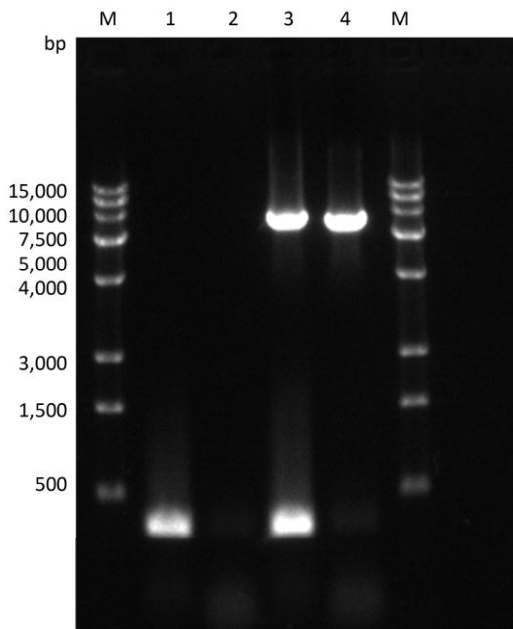
Supplementary Figure S3. Verification of PV1 genomic DNA with 1-124 nt region deleted. Lane M: DL15000 DNA markers (15,000, 10,000, 7,500, 5,000, 4,000, 3,000, 1,500, 500), PCR products of the full-length (integrated) PV1 genomic DNA (lane 3), and negative control (lane 1); PCR products of the PV1 genomic DNA lacking the 1-124 nt region (lane 4), and negative control (lane 2).

Supplementary Table S1. Primers Used to Amplify PV1 Genome

Primer Set	Primer Name	Sequence (5'→3')	Site (nt)
1	1F	TTAAAACAGCTCTGGGGT	1-18
	1R	TTTGGAGGCGTTACACTG	1,280-1,297
2	2F	CAATGCTAAACTCGCCAAAC	939-958
	2R	GATCCTGCCCAGTGTGTGT	2,086-2,104
3	3F	CCCATACTCTGCCTGTCACTC	2,006-2,026
	3R	CAGCCAAAATACCGAAGTC	3,185-3,203
4	4F	GCACTAGGTGACTCCCTC	3,146-3,163
	4R	TACGGTGTTTGCTCTTGAAC	4,462-4,481
5	5F	CAGGAACACCAGGAAATTCT	4,331-4,349
	5R	CAGTGGGAGGTTGATTCCAT	6,429-6,448
6	6F	TCTTGAACAAACAAACCAGAG	6,375-6,395
	6R	AAAAATTTACCCCTACAGCAGG	7,407-7,427
5'-NCR	5' -1[a]	CTTGGTTTTGTGCGTCTAAG	105-124
	5'-2F[b]	AGACGCACAAAACCAAGTT	108-126
	5'-2R	GAGCGAATCCAGCAAACAG	661-679
	5'-3[c]	CTGGATTCGCTCCATTGAG	669-686

Note. F, forward primer; R, reverse primer. [a]Amplification of the 1-124 nt region matched with primer 1F. [b]Amplification of the 108-679 nt region matched with 5'-2R. [c]Amplification of the 669-1,297 nt region matched with primer 1R.

Supplementary Table S2. Probes Used for Spot Hybridization Assays

Probe	Site (nt)	Sequence (5'→3')
1	1-40	GTGGGCCTCTGGGGTGGGTACAACCCCAGAGCTGTTTTAA
2	40-80	GCGTACAAGGGTACCGCAATACCGGAGTACTAGCCGCCACG
3	80-124	CTTGGTTTTGTGCGTCTAAGTTACGGGAAGGGAGTATAAAACAGG

Supplementary Table S3. Primers Used to Construct Damaged PV1 RNA

Primer name	Site (nt)	Sequence (5'→3')
F1	1-80	CCCGAAATTAATACGACTCACTATAGGTTAAAACAGCT CTGGGGTTGTACCCACCCCAGAGGCCCACGTGGCGG CTAGTACTCCGGTATTGCGGTACCCTTGTACGCCTTAAG
F2	1-20	CCCGAAATTAATACGACTCACTATAGGTTAAAACAGCTCTGGGGTTG
F3	125-144	CCGAATTCTCAAT AGAAG GGGGT ACAAA
TR	7,433-7,471	TTTTTTTTTTTTTTTTTTTTTTTTTTTTTTTTTCCTCCGAAT

Note. Primer pair F3/TR was used to amplify the 125-7,471 nt region; the obtained PCR products were ligated with F1 to construct PV1 lacking the 80-124 nt region. Primer pair F3/TR was used to construct PV1 lacking the 1-124 nt region. Primer pair F2/TR was used to construct complete PV1 genome.

Supplementary Table S4. Relationship between Ventilation Time and Ozone Concentration

Ventilation Time (s)	Ozone Concentration (mg/L)
0	0.00
30	0.60
60	1.08
90	1.44
105	1.44
120	1.44

Note. Water volume was 100 mL, flow rate of ozone was 0.5 L/min, and temperature was 20 °C.

Supplementary Table S5. Relationship between Ventilation Time, Ozone Concentration, and PV1 Inactivation Rate

Ventilation Time (s)	Ozone Concentration (mg/L)	Inactivation Rate (%)
0	0.00	0.0
30	0.00	66.7
60	0.00	99.0
90	0.06	99.9
105	0.12	100.0
120	0.22	100.0

Note. Water volume was 100 mL, initial concentration of PV1 was 10^6 PFU/L in the water sample, flow rate of ozone was 0.5 L/min, and temperature was 20 °C.

Supplementary Table S6. Spot Hybridization Assay to Detect Damage to the 1-124 nt Region in the 5'-NCR

Ventilation Time (s)	Infectivity	1-40	40-80	80-124
0	+	+	+	+
30	+	+	+	+
60	+	+	+	+
90	+	+	+	+
105	-	+	+	-
120	-	-	-	-

Note. +, Positive result; -, Negative result in replicate experiments (*n* = 3).